

Combined PSO-FDFD Optimization of Rectangular Ridged Waveguides

Marco Simone, Alessandro Fanti, Giorgio Montisci, Giovanni Andrea Casula,
and Giuseppe Mazzarella

Dipartimento di Ingegneria Elettrica ed Elettronica
Università di Cagliari, Cagliari, Italy

marco.simone@diee.unica.it, alessandro.fanti@diee.unica.it, giorgio.montisci@unica.it, a.casula@diee.unica.it,
mazzarella@diee.unica.it

Abstract — Finite-difference frequency-domain technique in conjunction with the particle swarm optimization algorithm is presented as an effective procedure for ridged waveguides design optimization. A suitable objective function is furthermore able to deal with the conflicting requirements of wide bandwidth and high power handling capability. Different configurations have been analyzed, and the influence of the algorithm parameters on the optimized structure has been investigated.

Index Terms — Cutoff frequency, finite-difference frequency-domain, microwave components, microwave filters, optimization, PSO, ridged waveguides, waveguide modes.

I. INTRODUCTION

In RF engineering, a large number of applications require very intense fields, thus devices with high power handling capabilities and low losses are required. Metallic hollow waveguides (WGs) represent the structures more suitable to satisfy such strict requirements. WG modal propagation is high-pass and dispersive [1], so WGs can be used only in the frequency range characterized by single-mode propagation. Such a useful bandwidth (BW) is relatively narrow. Ridged waveguide (R-WG) structures have been proposed to increase significantly the BW, retaining all the useful WG properties [2].

The first approach to the electromagnetic analysis of rectangular R-WG [3,4] is the transverse resonance technique (TRT) [5]. TRT is able to compute, in an approximate way, the cut-off frequencies of the first few modes of a R-WG and their attenuation. Moreover, Hopfer [4] was able to compute also the power handling capability (PHC) taking also into account, in an approximate way, the singular behaviour of the field at the wedges.

Despite of the reduced accuracy, TRT is still a useful tool for the “back-to-envelope” evaluation of the cut-off frequency of the fundamental mode [6]. But, of

course, numerical techniques such as finite-difference frequency-domain (FDFD) [7] or finite element method (FEM) [8] allow to compute the cut-off frequencies and the modal distribution of a R-WG with a far better accuracy. On the other hand, the accuracy of TRT is sufficient to compute the PHC of a R-WG [4].

In practical applications, the increase in BW comes together with a reduced PHC of R-WGs which can limit their use. In other words, we have to deal with two conflicting requirements. Suitable optimization procedures are therefore needed in order to obtain an effective trade-off. Such procedures are based on a synergic work of a time-effective EM analysis program of the structure and of a suitable optimization algorithm.

In this work, an effective in-house FDFD-TRT procedure has been developed to compute eigenvalues, mode distribution and PHC of different R-WG configurations, whereas the optimization problem has been solved by using the particle swarm optimization (PSO) algorithm. In the following section the procedure is described in detail.

We have considered different ridged configurations with different design specifications, extending therefore the results presented in [9].

II. FDFD

The R-WG analysis procedure is realized using a FDFD strategy [7], which can be applied both to scalar [10]-[12] and vector [13] problems. As a matter of fact, the FDFD approach, namely the direct discretization of the differential eigenvalue problem, is the simplest numerical strategy to compute eigenvalues and modes of metallic hollow WGs [14]. Therefore, it is well tailored to be used in PSO, but it is useful also in the procedures based on method of moments (MoM) [15]-[16] or mode-matching (MM) [17]. The WG section is partitioned in a set of regular discretization cells, and the differential eigenvalue problem [18] is replaced by a finite difference one, using suitable Taylor approximations of second [7] or fourth [19] order. The standard FDFD approach, using two Cartesian sampling grids (one for

TE modes and the other for TM, due to the different boundary conditions), allows a very effective solution for rectangular WGs or, more generally, for WGs with piecewise rectangular boundaries, since in these cases the boundary is perfectly fitted to the grid, either uniform or non-uniform. The FDFD has been suitably generalized [20] to evaluate all modes (either TE or TM) on a single grid. The discretization results in a matrix eigenvalue problem, which is sparse, so a very effective computation is possible. Once the eigenvalue problem is solved, the smallest two eigenvalues give directly the BW.

III. PSO

PSO is an iterative algorithm designed to find out the solution of optimization problems, very efficient in solving multidimensional problems in a large variety of applications. It has been proposed first by Kennedy and Eberhart [21] for non-linear functions optimization and neural network training. Later on, it has been introduced in electromagnetic research for antenna design [22]-[25], and subsequently it has been applied to artificial ground plane for surface wave antennas [26], microstrip antennas [27]-[29], linear and planar array geometry [30]-[31], log-periodic array dipole antennas, aperture antennas, and so on.

PSO takes inspiration from the animal kingdom, in particular from the group movement in search of a common objective. The algorithm consists of a swarm randomly initialized inside a predetermined solution space, which represents the set of the admissible solutions for the problem. The quality of the solution is measured through a suitable objective function, associated with each position in the solution space. The choice of the objective function is a key point of every PSO procedure, since it must be accurately defined to well describe the requests of the problem. The group of particles moves iteratively inside the solution space, trying to reach the position which represents the optimal solution, corresponding to the minimum value of the objective function. The movement of each individual is based on its own instinct, on the memory of its path and on the iterations with the other individuals. Each particle is described by a vector of variables x , which are the coordinates of the solution space and, at the same time, the parameters to be optimized. In the j -th iteration, the i -th particle is characterized by its position $x_{i,j}$ (1) and velocity $v_{i,j}$ (2). Next position, direction and velocity of the single particle are updated according to its position and velocity at the previous step, the best solution found by the particle in its path (personal best, p), and the best solution found by the whole swarm (global best, g).

Therefore,

$$x_{i,j} = x_{i,j-1} + v_{i,j}, \quad (1)$$

$$v_{i,j} = w \cdot v_{i,j-1} + c_1 \cdot r_1 \cdot (p_{i,j} - x_{i,j-1}) + c_2 \cdot r_2 \cdot (g_{i,j} - x_{i,j-1}), \quad (2)$$

wherein, w scales the velocity component in the same direction of the previous step (inertia weight), r_1, r_2 are two random numbers between 0.0 and 1.0 which simulate the random component of the swarm behaviour, c_1, c_2 provide a weight between the pull of g and p : low values allow particles to roam far from target positions before being attracted to, whereas high values provide movements more strongly orientated towards the target. Eberhart suggested that the best choice for c_1 and c_2 is 2.0 [32] for most of applications. In general, velocity is applied to position updating for a time-step Δt which is set to 1 in this work.

The main steps of the algorithm can be indentified in the following (Fig. 1):

1. Initialization of swarm position and velocity;
2. Systematic particles movement in the solution space. For each particle:
 - a) Objective function fitness evaluation (g, p update)
 - b) Velocity update
 - c) Position update (swarm movement);
3. Iteration of point 2 until a stop criterion (convergence or maximum number of iterations) is reached.

The objective function shown in Fig. 1 is relative to the model proposed in this paper and evaluates the performance of the R-WG, whose geometrical parameters constitute the x vector components, and therefore the dimensions of the solution space.

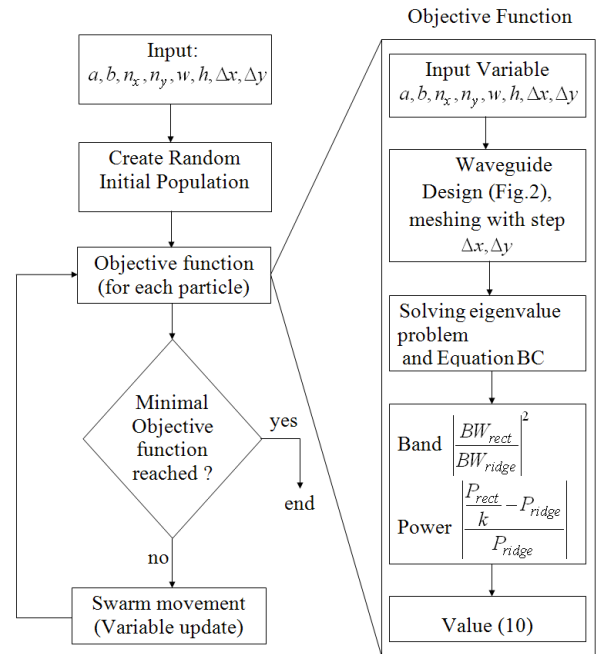


Fig. 1. PSO block diagram.

IV. WG DESIGN

The implementation of an optimization algorithm starts from the definition of the optimization variables, which define the solution space through their constraints. In our case, the variables are the geometrical dimensions of all the ridges (width w and height h) and the horizontal spacing s between them. However, use of FDFD requires the WG section be discretized. As a consequence, the variables can assume only values that are multiples of the discretization steps (D_x, D_y) of the WG section. The solution space of the PSO is therefore a discrete one, and its constraints are set to prevent all singular configurations. Four different R-WG configurations have been considered, with either equal or unequal ridges, and are shown in Fig. 2.

V. EVALUATION OF POWER HANDLING CAPABILITY

The PHC depends on both the WG shape and, for hollow WGs, the dielectric capability of the air. In order to compare different R-WGs, the maximum value of $|E|$ has been set to 1. Following Hopfer [4], we start from the well known relation between the power flux P and the total energy for unit length W_{EM} :

$$P = W_{EM} \frac{\beta c}{k_0}, \quad (3)$$

wherein β is the propagation constant, c and k_0 are respectively the speed of light and the wavenumber in vacuum. Then we obtain:

$$P = \frac{1}{\sqrt{\epsilon_0 \mu_0}} \frac{\lambda_0}{\lambda_g} \left[2 \left(\frac{1}{2} CV^2 \right) + \frac{\epsilon_0}{2} \int E^2 dS \right], \quad (4)$$

where V is the fundamental mode voltage at the ridge edge, and C is the capacitance equivalent to each discontinuity:

$$C = \frac{2\epsilon_0}{\pi} \ln \left[\csc \left(\frac{\pi d}{2b} \right) \right], \quad (5)$$

wherein b is the height of the waveguide, and d is the height of the ridged area.

The total energy can be evaluated on the transmission-line equivalent circuit used for TRT. Since the details of the configurations 1 (Fig. 2 (a)) and 2 (Fig. 2 (b)) are discussed in an appendix of [4], we add here some considerations for the six-ridges case (shown in Fig. 2 (c)), since the generalization is not trivial. Figure 3 represents the transmission line model (TLM) of only half of the transversal section of a six-ridge WG, so it stores half of the total energy. The antipodal case (shown in Fig. 2 (d)) can be dealt with in the same way.

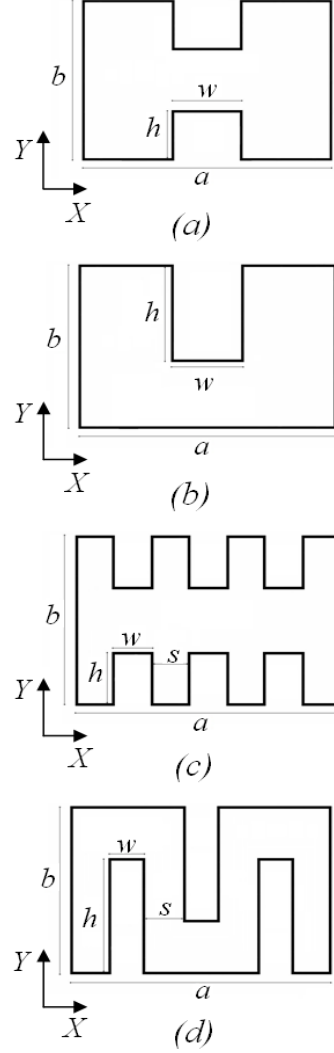


Fig. 2. (a) Configuration 1: a standard R-WG with two ridges centred along the widths of a rectangular WG; (b) configuration 2: a standard R-WG with a ridge centred along a width of a rectangular WG; (c) configuration 3: a standard R-WG with six ridges with equispaced centres; (d) configuration 4: a three-symmetric-antipodal R-WG.

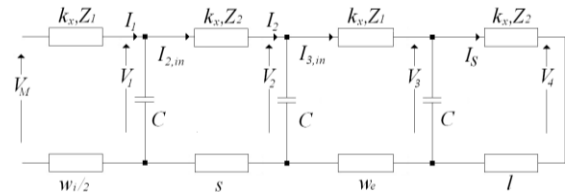


Fig. 3. Transmission line model for a six ridges geometry.

The TRT starts by considering the transversal section of the R-WG as a resonator. The propagation constant is the same for each line (representing a parallel plate section of the R-WG) and it is equal to the transverse propagation constant k_c , while the impedance is proportional to the WG height. To evaluate the PHC, a voltage V_M corresponding to the maximum electric field is set at the open-circuit (i.e., at the WG center), and an unknown current I_S at the short circuit end (i.e., at the WG lateral wall).

Letting $l_1 = w_i/2$, $l_2 = s$, we have:

$$\begin{aligned} V_1 &= A_1 \cos(k_x x) \\ V_2 &= A_2 \cos[k_x(x-l_1)] - jB_2 \sin[k_x(x-l_1)] \\ V_3 &= A_3 \cos[k_x(x-(l_1+l_2))] + \\ &\quad - jB_3 \sin[k_x(x-(l_1+l_2))] \\ V_4 &= B_4 \sin(k_x x) \end{aligned}, \quad (6)$$

where k_x is the propagation constant in the x direction at cutoff and is given by $k_x = k_c = 2\pi/\lambda_c$ and,

$$\begin{aligned} A_1 &= V_M \\ A_2 &= V_1(w_i/2) \\ A_3 &= V_2(w_i/2 + s), \\ B_2 &= -jZ_2 I_{2,in} \\ B_3 &= -jZ_1 I_{3,in} \\ B_4 &= -jZ_2 I_S \end{aligned}, \quad (7)$$

$I_{2,in}$, $I_{3,in}$ are the input currents at the lines after the capacitors nodes:

$$\begin{aligned} I_1(w_i/2) &= I_{2,in} - CV_1(w_i/2) \\ I_2(w_i/2 + s) &= I_{3,in} - CV_2(w_i/2 + s). \end{aligned} \quad (8)$$

The unknown current I_S can be obtained by imposing the continuity of the voltages at the steps. The electric field is described from the (6) as:

$$\begin{aligned} E_1 &= G_1 V_1 \\ E_2 &= G_2 V_2 \\ E_3 &= G_3 V_3, \\ E_4 &= G_4 V_4 \end{aligned}, \quad (9)$$

the constants G_1 , G_2 , G_3 , G_4 can be obtained by imposing the voltage continuity at the steps.

VI. RESULTS

A. FDFD and PSO parameters

A 6x2 cm WG has been considered for all cases of Fig. 2. The WG cross-section has been discretized using a TE grid with steps $(D_x, D_y) = 0.1 \text{ mm}$. It follows that the dimensions w , h , and s are expressed in terms of number of nodes in the grid. The structure has been tested for different values of acceleration coefficient and number of particles np (i.e., the swarm size), and it has

been verified whether different PSO parameters modify or not the results. In all the tests, a varying inertia weight is applied by linearly changing its value from 0.9 at the beginning of the iterations to 0.4 towards the end (a smaller inertia weight encourages the local search [33]). We will show the optimal bandwidth $BW = f_{c2} - f_{c1}$, and the ratio BW_N between the bandwidth of the optimal R-WG and of the rectangular one with the same external size. f_{c1} , f_{c2} are the cut-off frequencies of the first two R-WG modes.

B. Objective functions

An appropriate objective function must be defined to obtain the solution best suited to the required application. It has been selected an objective function able to optimize the BW with a constraint on the power. More precisely, the following objective function:

$$f(k) = \left| \frac{P_{rect}/k - P_{ridge}}{P_{ridge}} \right| + \left| \frac{BW_{rect}}{BW_{ridge}} \right|^2, \quad (10)$$

maximizes the BW with a constraint on the power decrease (k-time reduction with respect to the rectangular WG). P_{ridge} , BW_{ridge} are the values for the R-WG at hand, whereas P_{rect} , BW_{rect} are the values for the host rectangular WG [34]. In the following, it has been usually chosen $k = 2.0$; 3.0 , so that the objective function tries to optimize the BW with a maximum power reduction equal to 50% or 66%.

C. Convergence test

The behaviour of a R-WG in terms of BW is rather well-known. Some preliminary optimization of $f(\infty)$ (i.e., BW-only optimization) have been then performed to evaluate the convergence properties of our approach. Since the solution space is discrete, we assume as convergence criterion the equality of the best and worst fitness values of the swarm.

A test on configuration 1 leads to the result that the largest BW requires the highest possible ridges ($h = 99$) with a large width ($w = 192$). This optimum is always obtained using different c_1 , c_2 , np values and starting point, since no traps are present. The smaller c_i 's, the more rapid the convergence: for $np = 5$, the convergence require about 80 steps for $c_1 = c_2 = 1.5$, and about 100 steps for $c_1 = c_2 = 2$. A similar behaviour has been obtained for larger np . On the other hand, a larger c_i 's allow to better explore the solution space, and therefore to escape more easily from traps. The increase in the computational cost is quite small and, since the introduction of the PHC constraints modifies the topology of the solution space and can introduce some local minima (i.e., traps) we have, in the following, chosen $c_1 = c_2 = 2$.

Then, we have tested the dependence of the number of particles of the swarm. A typical value for np

is 1.5 to 2 times the number of optimization variables. Of course, for the simple cases involving only two variables, we have taken $np \geq 5$. It appears that a significant increase of np introduces no reduction in the number of iterative steps. Even worse, this number usually increases a little bit (10-30% in the cases we have tested). Therefore, we conclude that the typical value of np quoted above is also the more effective, since we need, at each step, np evaluation of eigenvalues and mode distributions.

D. Optimization results

The objective functions $f(2)$ and $f(3)$ have been chosen to constraint the ratio P_{ridge}/P_{rect} to 50% or 33% respectively. The tests confirm the effectiveness of the objective function: the constraint on PHC is fulfilled with a smaller discrepancy.

The optimized geometries of the configuration 1 have been obtained with $np = 5$ for equal ridges (2 optimization variables) and $np = 10$ for different ridges (4 variables), and they are shown in Table 1. Actually, the optimum is always with equal ridges, so that only this case is shown. The optimum BW should be compared with the best one obtained with no PHC constraints, which is equal to 6.7726 GHz (i.e., $BW_N = 2.711$), but in this case the maximum power flux is very small respect to P_{rect} .

Table 1: Results configuration 1

k	$\frac{w}{a}$	$\frac{h}{b}$	BW (GHz)	BW_N (GHz)
2	0.35	0.20	3.07	1.23
3	0.33	0.27	3.42	1.37

Similarly, the Table 2 presents the performance of the configuration 2. A single ridge presents a lower improvement in terms of bandwidth with respect to the 2-ridges case.

Table 2: Results configuration 2

k	$\frac{w}{a}$	$\frac{h}{b}$	BW (GHz)	BW_N (GHz)
2	0.28	0.37	3.00	1.20
3	0.26	0.52	3.29	1.32

The configurations 3, and 4 investigate the effect of the side ridges. The configuration 3 does not work for the equal ridges case: as expected, large side ridges prevent the BW improvement, so the algorithm tends to remove them and the geometry tends toward rectangular WG without ridges. Regarding the case with different ridges, the symmetry of the fundamental mode allows to simplify the problem to a symmetric structure with respect to its two axes: it has been

considered a geometry whose central ridges (w_c, h_c) vary independently of the side ones (w_s, h_s), and the spacing between the ridges s is chosen as another parameter to be optimized. The solution space has therefore 5 dimensions and the optimized geometries (obtained with $np = 20$ particles in the swarm) are shown in Table 3. A comparison with Table 1 shows a significant BW improvement (for a given PHC) due to the additional (optimized) side ridges.

Table 3: Results configuration 3

k	$\frac{w_c}{a}, \frac{h_c}{b}$	$\frac{w_s}{a}, \frac{h_s}{b}$	$\frac{s}{a}$	BW (GHz)	BWN (GHz)
2	0.32, 0.38	0.32, 0.24	0.01	3.48	1.39
3	0.29, 0.36	0.32, 0.15	0.03	3.67	1.47

As a further analysis of the side ridges effect, we consider an antipodal geometry (configuration 4), where the two external ridges are equal and equally spaced from the central one. Such configuration can also be obtained by adding two lateral ridges to configuration 2 on the un-ridged side. Since the ridge spacing is also an optimization variable, the solution space has again 5 dimensions, and we have used $np = 20$ in the tests. Table 4 displays the performance of this geometry.

Table 4: Results configuration 4

k	$\frac{w_c}{a}, \frac{h_c}{b}$	$\frac{w_s}{a}, \frac{h_s}{b}$	$\frac{s}{a}$	BW (GHz)	BWN (GHz)
2	0.19, 0.46	0.03, 0.16	0.35	3.25	1.300
3	0.12, 0.47	0.03, 0.05	0.34	3.27	1.307

In both cases, the lateral ridges are small and distant from the central one and, unlike the configuration 2, the central ridge does not cross the horizontal axis of the WG. It is apparent from Table 4 that the antipodal configuration allows a BW improvement when a relatively loose constraint on PHC is set. For the tested case, a constraint of 50% reduction in power gives an improvement in BW around 10%. On the other hand, when a small PHC is required, the single ridge geometry is preferable.

VII. CONCLUSIONS

In this paper, the effectiveness of PSO in the geometrical optimization of a guiding structure has been illustrated. It has been shown how a suitable objective function allows to make a trade-off between two conflicting requests: the BW of a R-WG has been maximized for a determined power decrease respect to the un-ridged geometry. Among the different geometries presented, the 6-symmetric ridge geometry results to be the best solution in terms of bandwidth.

ACKNOWLEDGMENT

Marco Simone gratefully acknowledges Sardinia Regional Government for the financial support of his Ph.D. scholarship (P.O.R. Sardegna F.S.E. Operational Programme of the Autonomous Region of Sardinia, European Social Fund 2007-2013 - Axis IV Human Resources, Objective I.3, Line of Activity I.3.1.).

Alessandro Fanti gratefully acknowledges Sardinia Regional Government for the financial support (P.O.R. Sardegna F.S.E. Operational Programme of the Autonomous Region of Sardinia, European Social Fund 2007-2013 - Axis IV Human Resources, Objective I.3, Line of Activity I.3.1 Avviso di chiamata per il finanziamento di Assegni di Ricerca).

This work was supported in part by Regione Autonoma della Sardegna under contract CRP-49231 (CUP C45E120000200002).

The authors would like to thank George Evers for making freely available its MATLAB PSO Research Toolbox which has been used for simulations.

REFERENCES

- [1] R. E. Collin, *Field Theory of Guided Waves*, 2nd ed., New York, IEEE Press, 1991.
- [2] J. Helszajn, *Ridge Waveguides and Passive Microwave Components*, London, IEE, 2000.
- [3] S. B. Cohn, "Properties of ridged waveguide," *Proceedings of the IRE*, vol. 35, pp. 783-788, Aug. 1947.
- [4] S. Hopfer, "The design of ridge waveguide," *IRE Transactions on Microwave Theory and Techniques*, vol. MTT-3, pp. 20-29, Oct. 1955.
- [5] R. Sorrentino, *Transverse Resonance Technique*, in *Numerical Techniques for Microwave and Millimeter Wave Passive Structures*, Chapter 11, New York, John Wiley, 1989.
- [6] J. Helszajn and M. McKay, "Voltage-current definition of impedance of double ridge waveguide using the finite element method," *IEE Proc.-Microw. Antennas Propagation*, vol. 145, no. 1, Feb. 1998.
- [7] A. Fanti and G. Mazzarella, "Curvilinear finite difference approach to the computation of modes of circular and elliptic waveguides," *IEEE Proc. Int. Conf. on Applied Electromagnetics and Communications, (ICECom 2010)*, Dubrovnik, Croazia, Sep. 20-23, 2010.
- [8] A. M. Svedin, "Propagation analysis of chiro waveguides using the finite element method," *IEEE Trans. on Microwave Theory Tech.*, vol. 38, no. 10, pp. 1488-1496, Oct. 1990.
- [9] M. Simone, A. Fanti, G. Mazzarella, and G. Montisci, "Band optimization of ridge waveguides using PSO," *30th International Review of Progress in Applied Computational Electromagnetics*, Jacksonville, Florida, Mar. 23-27, 2014.
- [10] A. Fanti, L. Deias, G. A. Casula, and G. Montisci, "A fourth order FDFD approach for the analysis of sectorial elliptic waveguides," *Applied Computational Electromagnetics Society (ACES) Journal*, vol. 30, no. 5, pp. 488-495, May 2015.
- [11] C. S. Lavranos and G. A. Kyriacou, "Eigenvalue analysis of curved waveguides employing FDFD method in orthogonal curvilinear co-ordinates," *IEE Electronics Letters*, vol. 42, no. 12, pp. 702-704, June 2006.
- [12] C. S. Lavranos and G. A. Kyriacou, "Eigenvalue analysis of curved waveguides employing an orthogonal curvilinear frequency-domain finite-difference method," *IEEE Transactions on Microwave Theory and Techniques*, vol. 57, iss. 3, pp. 594-611, Mar. 2009.
- [13] A. Fanti, G. Mazzarella, G. Montisci, and G. A. Casula, "VFD approach to the computation TE and TM modes in elliptic waveguide on TM grid," *Applied Computational Electromagnetics Society (ACES) Journal*, vol. 28, pp. 1205-1212, 2013.
- [14] Y. J. Zhao, K. L. Wu, and K. K. M. Cheng, "A compact 2-D full-wave finite-difference frequency-domain method for general guided wave structures," *IEEE Transactions on Microwave Theory and Techniques*, vol. 50, iss. 7, pp. 1844-1848, 2002.
- [15] G. Mazzarella and G. Montisci, "Accurate characterization of the interaction between coupling slots and waveguide bends in waveguide slot arrays," *IEEE Trans. Microw. Theory Tech.*, vol. MTT 48, pp. 1154-1157, Sep. 2000.
- [16] T. Hirano, J. Hirokawa, and M. Ando, "Method of moments analysis of a waveguide crossed slot by using the eigenmode basis functions derived by the edge-based nite-element," *Proc. Inst. Elect. Eng. Microwaves, Antennas Propagation*, vol. 147, no. 5, pp. 349-353, 2000.
- [17] J. Bornemann and F. Taringou, "Mode-matching analysis of substrate-integrated waveguide circuits," *Proc. Canadian Conf. Elec. Comp. Engr.*, pp. 579-582, Niagara Falls, Canada, May 2011.
- [18] K. W. Morton and D. F. Mayers, *Numerical Solution of Partial Differential Equations, An Introduction*, Cambridge University Press, 2005.
- [19] A. Fanti, M. Simone, and G. Mazzarella, "High order FDFD computation of all waveguide modes using a single grid," *IEEE Int. Proc. 2013 Loughborough Antennas and Propagation Conference*, Loughborough, UK, 2013.
- [20] A. Fanti and G. Mazzarella, "Finite difference single grid evaluation of TE and TM modes in metallic waveguides," *IEEE Proc. Int. Conf. Loughborough Antennas and Propagation Conference*, UK, pp. 517-520, Nov. 8-9, 2010.
- [21] J. Kennedy and R. Eberhart, "Particle swarm

- optimization,” *Proceedings of IEEE International Conference on Neural Networks*, vol. 4, pp. 1942-1948, Perth Wash, Australia, Nov. 1995.
- [22] J. Robinson, S. Sinton, and Y. Rahmat-Samii, “Particle swarm, genetic algorithm, and their hybrids: optimization of a profiled corrugated horn antenna,” *IEEE Antennas and Propagation Society International Symposium 2002*, vol. 1, pp. 314-317, San Antonio, Texas, June 2002.
- [23] J. Robinson and Y. Rahmat-Samii, “Particle swarm optimization in electromagnetics,” *IEEE Transactions on Antennas and Propagation*, vol. 52, iss. 2, pp. 397-407, Feb. 2004.
- [24] N. Jin and Y. Rahmat-Samii, “Particle swarm optimization for antenna designs in engineering electromagnetics,” *Journal of Artificial Evolution and Applications*, vol. 2008, no. 9, 2008.
- [25] H. Wu, J. Geng, R. Jin, J. Qiu, W. Liu, J. Chen, and S. Liu, “An improved comprehensive learning particle swarm optimization and its application to the semiautomatic design of antennas,” *IEEE Transactions on Antennas and Propagation*, vol. 57, iss. 10, pp. 3018-3028, Oct. 2009.
- [26] E. Carrubba, A. Junge, F. Marliani, and A. Monorchio, “Particle swarm optimization for multiple dipole modeling of space equipment,” *IEEE Transactions on Magnetics*, vol. 50, iss. 12, pp. 1-10, Dec. 2014.
- [27] Y. Choukiker, S. K. Behera, D. Mishra, and R. K. Mishra, “Optimization of dual band microstrip antenna using PSO,” *Applied Electromagnetics Conference (AEMC)*, Kolkata, India, pp. 1-4, Dec. 2009.
- [28] A. A. Minasian and T. S. Bird, “Particle swarm optimization of microstrip antennas for wireless communication systems,” *IEEE Transactions on Antennas and Propagation*, vol. 61, iss. 12, pp. 6214-6217, Dec. 2013.
- [29] A. Deb, J. S. Roy, and B. Gupta, “Performance comparison of differential evolution, particle swarm optimization and genetic algorithm in the design of circularly polarized microstrip antennas,” *IEEE Transactions on Antennas and Propagation*, vol. 62, iss. 8, pp. 3920-3928, Aug. 2014.
- [30] M. M. Khodier and C. G. Christodoulou, “Linear array geometry synthesis with minimum side lobe level and null control using particle swarm optimization,” *IEEE Transactions on Antennas and Propagation*, vol. 53, iss. 8, part 2, pp. 2674-2679, Aug. 2005.
- [31] D. Cao, A. Modiri, G. Sureka, and K. Kiasaleh, “DSP implementation of the particle swarm and genetic algorithms for real time design of thinned array antennas,” *IEEE Antennas Wireless Propagation Letter*, vol. 11, pp. 1170-1173, 2012.
- [32] R. C. Eberhart and Y. Shi, “Particle swarm optimization: development, applications and resources,” *Proceedings of the 2001 Congress on Evolutionary Computation*, COEX Seoul, Korea, vol. 1, pp. 81-86, May 2001.
- [33] Y. Shi and R. Eberhart, “Empirical study of particle swarm optimization,” *Proceedings of the IEEE Congress on Evolutionary Computation*, vol. 3, pp. 1945-1950, 1999.
- [34] M. Simone, A. Fanti, and G. Mazzarella, “Ridge waveguide optimization with PSO algorithm,” *Journal of Electromagnetic Waves and Applications*, vol. 2, iss. 29, pp. 199-209, Feb. 2015.



Marco Simone received the bachelor's degree in Electronics Engineering from the University of Cagliari in 2007. In 2011, he received the master's degree from the University of Cagliari. In 2012, he did an internship at Vitrociset about Radar Systems, Radar Signal and Data Processing. From 2013 to 2015, he worked as Ph.D. student (scholarship winner) at Doctoral School of Electronic and Computer Engineering (DRIE) at the Department of Electrical and Electronic Engineering (DIEE) of University of Cagliari. He's currently writing his Ph.D. thesis (to be discussed in March). In 2015, he spent 6 months at Queen Mary University of London to achieve the Doctor Europaeus qualification. From January 2016, he is employed as Postdoctoral Research Assistant in the School of Electronic Engineering and Computer Science at Queen Mary University of London, under the supervision of Prof. Yang Hao. His research activity involves the use of optimization techniques for microwave devices.



Alessandro Fanti received the Laurea degree in Electronic Engineering and Ph.D. degree in Electronic Engineering and Computer Science from the University of Cagliari in 2006 and 2012, respectively. He currently holds a post-doc scholarship for design of microwave components. His research activity involves the use of numerical techniques for modes computation of guiding structures, optimization techniques, analysis and design of waveguide slot arrays, analysis and design of patch antennas.



Giorgio Montisci received the Laurea degree (summa cum laude) in Electronic Engineering and Ph.D. degree in Electronic Engineering and Computer Science from the University of Cagliari, Cagliari, Italy, in 1997 and 2000, respectively.

In November 2000, he became Assistant Professor, and since October 2015 he is Associate Professor of Electromagnetic Fields at the Dipartimento di Ingegneria Elettrica ed Elettronica, University of Cagliari, teaching courses in electromagnetics and microwave engineering. His research activity is mainly focused on analysis and design of waveguide slot arrays, microwave holographic techniques for the diagnostic of large reflector antennas, numerical methods in electromagnetics, and printed antennas. He is author or co-author of about 50 papers in international journals and Reviewer for EM Journals.



Giovanni Andrea Casula received the Laurea degree (summa cum laude) in Electronic Engineering and Ph.D. degree in Electronic Engineering and Computer Science from the University di Cagliari, Cagliari, Italy, in 2000 and 2004, respectively. Since March 2006, he

is an Assistant Professor of Electromagnetic Field and Microwave Engineering at the Dipartimento di Ingegneria Elettrica ed Elettronica, University of Cagliari. His current research interests are in the field of synthesis, analysis and design of wire, patch, and slot antennas. Casula serves as Reviewer for several international journals and is a Member of the Italian Electromagnetic Society (SIEm).



Giuseppe Mazzarella graduated Summa with Laude in Electronic Engineering from the Università “Federico II” of Naples in 1984 and obtained the Ph.D. in Electronic Engineering and Computer Science in 1989. In 1990, he became Assistant Professor at the

Dipartimento di Ingegneria Elettronica at the Università “Federico II” of Naples. Since 1992, he is with the Dipartimento di Ingegneria Elettrica ed Elettronica of the Universit di Cagliari, first as Associate Professor and then, since 2000, as Full Professor, teaching courses in Electromagnetics, Microwave, Antennas and Remote Sensing. His research activity has focused mainly on: efficient synthesis of large arrays of slots, power synthesis of array factor, microwave holography techniques for the diagnostic of large reflector antennas, use of evolutionary programming for inverse problems solving. He is author (or co-author) of about 50 papers in international journals, and is a Reviewer for many EM journals.